Coordination Chemistry Reviews, 100 (1990) 67–103
Elsevier Science Publishers B.V., Amsterdam – Printed in The Netherlands

SPECTROSCOPIC STUDIES ON Cu_2Zn_2SOD: A CONTINUOUS ADVANCEMENT OF INVESTIGATION TOOLS

IVANO BERTINI, LUCIA BANCI and MARIO PICCIOLI

Department of Chemistry, University of Florence, Via Gino Capponi 7, 50121 Florence (Italy)

CLAUDIO LUCHINAT

Institute of Agricultural Chemistry, University of Bologna, Viale Berti Pichat 10, 40127 Bologna (Italy)

(Received 27 April 1989)

CONTENTS

A. INTRODUCTION

The enzyme superoxide dismutase (SOD) was first discovered by Mann and Keilin in 1938 in bovine erythrocytes [1]. Owing to its apparent absence of activity and to the fact that it contained copper, it was named hemocuprein. In 1970, Carrico and Deutsch [2] found evidence that the protein

0010-8545/90/$12.95

contains zinc as well as copper. They named the protein erythrocuprein. The presence of enzymatic activity was suggested by McCord and Fridovich [3] when evidence of superoxide dismutase activity was found during the preparation of carbonic anhydrase.

The physiological role of SOD has been a matter of debate [4–13]. In vitro it shows a very high catalytic activity relative to the dismutation of superoxide:

$$2O_2^- + 2H^+ \rightleftharpoons H_2O_2 + O_2 \qquad (1)$$

This reaction has $\Delta E^{0\prime} = 1.05$ V and a kinetic constant that is strongly pH dependent. It has a maximum of 2.5×10^7 M^{-1} s^{-1} at pH 4.8, i.e. at the pK_a of HO_2, decreases with pH with a linear dependence on $[H^+]$ and levels off at less than 1 M^{-1} s^{-1} around pH 13. At the physiological pH the kinetic constant is 2.5×10^5 M^{-1} [6,12].

The two half-reactions ($O_2 + e^- \rightarrow O_2^-$ and $O_2^- + 2H^+ + e^- \rightarrow H_2O_2$) have $E^{0\prime} = -0.16$ V and $E^{0\prime} = 0.89$ V vs. the normal hydrogen electrode (NHE) respectively [12,14]. Therefore any redox pair with a potential intermediate between the above two values can act as a catalyst for the dismutation reaction.

The high efficiency of SOD in the dismutation of superoxide ($k_{cat} = 1 \times 10^6$ s^{-1}, $K_m = 3.5 \times 10^{-3}$ M, at 5 °C, pH 9.3 [15]) may be related to the role of the active cavity which attracts anions inside and increases the affinity of superoxide towards copper. We shall now discuss the studies which have shed light on the structure of the active site, i.e. the copper site plus the residues in the active cavity.

(i) X-ray structure

The X-ray structure is available for the bovine isoenzyme (BeSOD) at 2.0 Å resolution [16]. The copper(II) ion is bound to four histidines, one of which binds the two metal ions (Fig. 1) *. The coordination of zinc(II) ion is completed by two more histidines and one aspartate residue. Copper(II) is solvent exposed [16,17]. One water molecule is located at a Cu–O distance of 2.8 Å, pointing towards Arg-143, and a second water molecule is at 3.5 Å [17]. The metal donor distances and angles are reported in Table 1.

* Throughout this review the amino-acid residues are numbered following the human isoenzyme sequence. The yeast enzyme follows the same numbering over all the region of interest for the active site. For the bovine enzyme, for which the X-ray structure is available, the actual numbering of the active site residues is two units lower.

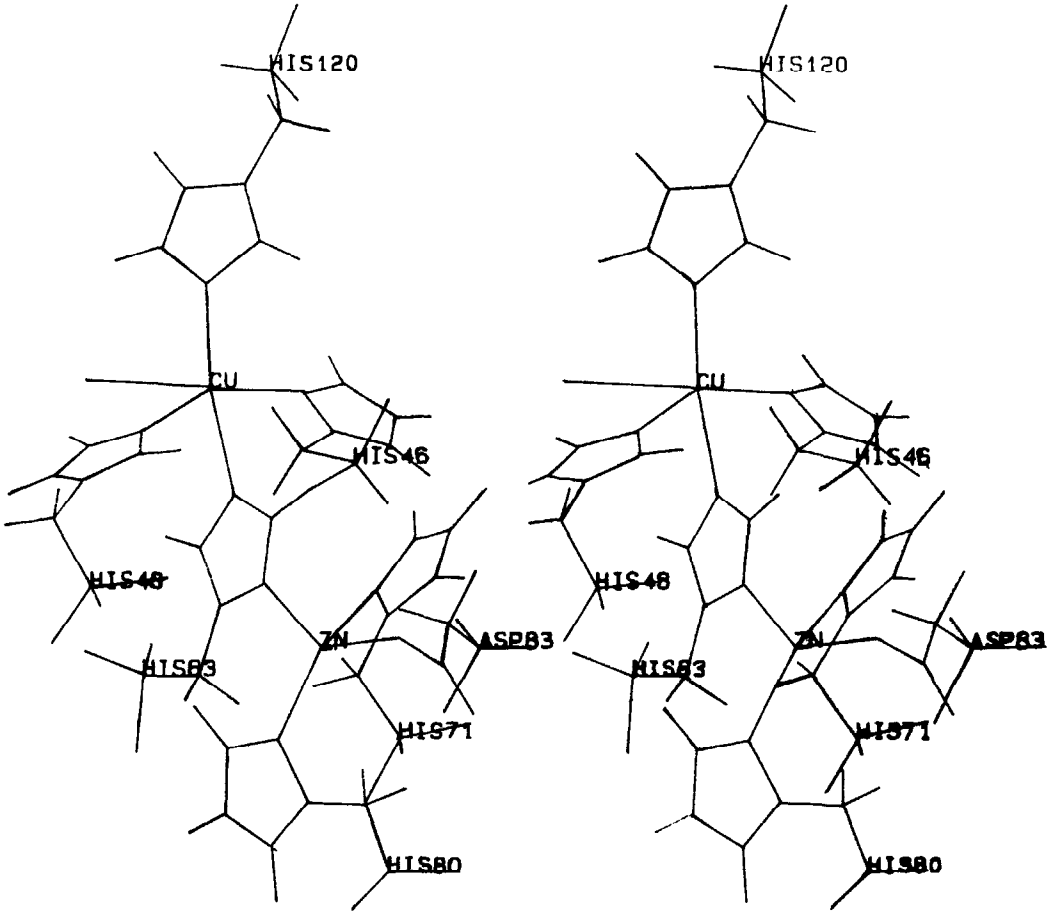

Fig. 1. Stereodrawing of the copper(II) and zinc(II) binding sites in SOD as deduced from the X-ray structure of the bovine isoenzyme [16]. The numbering of the residues is that of the human isoenzyme. Only the semicoordinated water 2.8 Å from copper(II) is shown.

TABLE 1

Ligand atom–metal ion distances and angles for the coordinated residues in BeSOD [a]

		Distance (Å)	Angle (deg)				
		Cu(II)	His-46 Nδ1	His-48 Nε2	His-120 Nε2	His-63 Nε2	H_2O
His-46	Nδ1	2.04	–	140	93	77	124
His-48	Nε2	2.14		–	117	82	93
His-120	Nε2	2.04			–	157	69
His-63	Nε2	2.06				–	100
H_2O		2.8					
		Zn(II)	His-63 Nδ1	His-71 Nδ1	His-80 Nδ1	Asp-83 Oγ	
His-63	Nδ1	2.06	–	113	113	117	
His-71	Nδ1	2.00		–	123	80	
His-80	Nδ1	2.94			–	107	
Asp-83	Oγ1	1.99					

[a] From ref. 17.

The metals are located in a cavity whose surface is about 10% of the total surface which is solvent exposed [17]. All the metal-binding ligand residues are conserved in all the different species for which amino-acid sequences

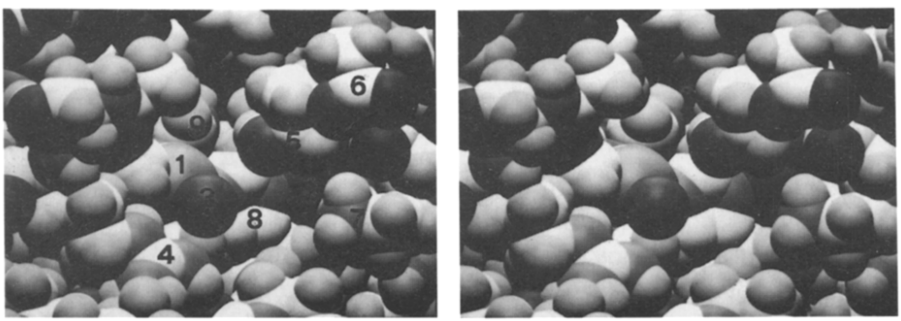

Fig. 2. Overall view of the active site cavity of SOD, based on the X-ray structure of the bovine enzyme [16] rendered as a CPK model. The site is viewed approximately from the outside. The numbers indicate relevant residues in the cavity. Besides the copper (1) and zinc (2) ions, the semicoordinated water molecule (3) is clearly visible, together with Arg-143 (4), Thr-137 (5) (with the hydroxo group hydrogen bonded either to the coordinated water, as in this scheme, or to Glu-133 (6)), Glu-133 (6), Lys-136 (7), the bridging imidazolato group of His-63 (8) and the edge of the copper-coordinated His-46 (9). Arg-143 and Thr-137 limit the inner volume of the cavity. Asp-124 (not visible) hydrogen-bridges the copper ligand His-46 to the zinc ligand His-71.

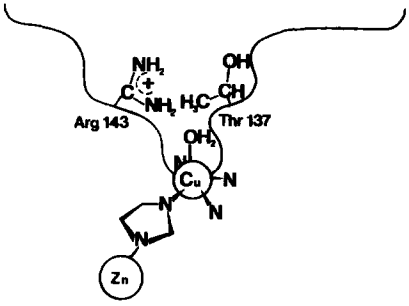

Fig. 3. Schematic drawing of the active site cavity, illustrating the positions of Arg-143 and Thr-137.

have been reported [13]. In addition, some other residues, present in the active cavity, are conserved in all the known Cu_2Zn_2SOD sequences, indicating that the conformation and the electrostatic forces of the active channel play a critical role in the enzymatic function [18,19]. Close to copper there are an arginine residue and a threonine residue (Arg-143 and Thr-137), which to some extent limit the access to the cavity (Figs. 2 and 3). Arg-143 has an important role in the enzymatic catalysis, possibly attracting superoxide inside the channel. Thr-137 is important for the hydrophylic character of the cavity; it is possibly involved in hydrogen bonding with Glu-133 [17]. It has been proposed that Lys-136 is responsible for the high pH pK_a of the enzymatic activity [20]. Asp-124 plays an important role in the structure of the cavity, because it bridges, through hydrogen bonds, His-46 (coordinated to copper) and His-71 (coordinated to zinc). The copper ion constitutes the floor of the cavity, together with the residues directly coordinated to it (His-46, His-48, His-63, His-120).

(ii) About the various derivatives

Cu_2Zn_2SOD is very widespread among living systems, from mammals to yeast. Among these isoenzymes, bovine, human and yeast SOD (BeSOD, HeSOD and YSOD) are the most studied. All the isoenzymes have very high homology, in particular some relevant groups such as Arg-143 and Asp-124 are preserved [13,21–23].

Other Cu_2Zn_2SODs in mammals, plants and other living systems have been described [24] and are currently being characterized.

(a) Metal substitution

The metal ions can be removed by dialysis at pH 3.8 against a metal chelator such as ethylenediaminetetraacetic acid (EDTA) [3,25,26]. The

TABLE 2

Superoxide dismutase activities of metal-substituted derivatives of BeSOD [a]

Derivative	Activity (% of native)	References
$Cu(II)_2Zn(II)_2$ as isolated	100	3, 4
$Cu(II)_2Zn(II)_2$ reconstituted	110	27
E_2E_2	< 0.1	3, 27
$E_2Co(II)_2$	0	32
$E_2Zn(II)_2$	0	38
$Cu(II)_2E_2$	20–80	27, 30
$Cu(II)_2Co(II)_2$	90	27
$Cu(II)_2Hg(II)_2$	90	27
$Cu(II)_2Cd(II)_2$	70	27
$Ag(I)_2Cu(II)_2$	5	39
$Ag(I)_2Co(II)_2$	Trace	39
$Cu(II)_2Cu(II)_2$	100	30
$Cu(II)_2Ni(II)_2$	30	29
$Ni(II)_2Co(II)_2$	Trace	37

[a] Adapted from ref. 9.

ternary and quaternary structures are maintained. At pH 3.8, by adding Cu^{2+}, Cu_2E_2SOD (E-empty) is obtained [27,28]. By raising the pH, other metal ions such as Co^{2+}, Ni^{2+}, Hg^{2+}, Cd^{2+} and Cu^{2+} can bind at the zinc site [27–30]. Alternatively, at pH about 6, many metal ions such as Zn^{2+}, Co^{2+}, Hg^{2+} and Cd^{2+} bind the apoenzyme at the zinc site to give E_2M_2SOD derivatives [31–34]. To the latter, metal ions such as Cu^{2+}, Co^{2+}, Zn^{2+}, Ni^{2+} can be added; they bind specifically to the copper site [31,32,35–37]. Valentine and coworkers have extensively exploited metal substitution techniques [9,28,29,31]. Therefore many metal-substituted derivatives are known and these are listed in Table 2. The activity is maintained only in the cases in which copper(II) is bound at the native enzyme copper(II) site [3,4,27,29,30,32,38,39]. Cobalt(II) at the copper site has the same coordination arrangement with five donor groups; however, when phosphate is present the bridge between cobalt and zinc is broken and the coordination around cobalt is provided by three histidines and phosphate itself [40,41]. Copper(II) in the native site can be reduced in vitro to copper(I). This derivative is fully active [42–44]. It is widely believed (see later) that the protein goes through an oxidation–reduction cycle during turnover. Valentine and coworkers have extensively characterized the thermal stability of SOD both in the absence and in the presence of various metal ions. The apoprotein is much less stable than the metal-substituted derivatives. $Cu^{I}_2Zn_2SOD$ is slightly more stable than $Cu^{II}_2Zn_2SOD$ [45].

(b) Anion derivatives

The anions CN^-, N_3^-, NCO^-, NCS^-, Cl^- and F^- are reported to bind the protein at the copper ion [46–48] and some of them (CN^-, F^-, N_3^-) are reported to inhibit catalytic activity. The inhibition is competitive [15,48,49]. NCO^- and NCS^- are not inhibitors [50,51]. There is ample evidence that anions are able to bind both copper(II) and copper(I) [46–53], although with a higher affinity for the former [15]. Therefore competitive inhibition could mean direct competition with superoxide for the metal-binding site. However, the results are equally consistent with anions altering the redox potential of the adduct to the point that it no longer reacts with superoxide. A marked change in redox potential has been observed in the cyanide derivative [54].

(c) Site-directed mutagenesis

Several SODs have been cloned; human erythrocyte SOD (HeSOD) has been cloned and expressed in both yeast and *E. coli* (HYSOD and HEcSOD respectively) [55,56]. As part of research intended to elucidate the relationship between structure and function of the enzyme, some key amino-acid residues have been changed by site-directed mutagenesis on the human isoenzyme. Some changes have been performed, either as single mutations of the wild type HSOD (WT HSOD), or on a mutant in which two cysteines, Cys-6 and Cys-111, have been substituted with an alanine and a serine respectively, in order to increase the thermostability of the enzyme. The Ala-6,Ser-111 derivative, AS HSOD, was shown to be practically identical with the WT HSOD as far as the enzymatic activity [57] and the structure of the active cavity [58] were concerned.

The mutants investigated up to now by physicochemical studies concern the amino-acid positions 137 and 143. Native Thr-137 has been substituted with isoleucine [59], Arg-143 has been substituted with isoleucine, lysine and glutamate [60,61]. Mutants on other residues in the active cavity have been prepared (Ser-137, Ala-137, Gln-132, Gln-133, Gln-132Gln-133, Ala-136, Gln-136, Asn-124, Gly-124, Asn-124Asn-125) but have not yet been fully investigated [62].

(iii) Aim of the review

Here we should like to review the spectroscopic properties of copper(II) in the above derivatives. They are peculiar because the coordination geometry of the metal is unprecedented in inorganic chemistry. If we understand the spectral parameters, then we can attempt to establish a relationship between spectroscopy and structure under the various conditions, and finally can contribute to the understanding of the catalytic cycle. We should like to

stress that advancement of theories and techniques have allowed us to know more about the protein. Besides the less traditional electron nuclear double resonance (ENDOR), electron spin echo (ESE) and water ^1H nuclear magnetic relaxation dispersion (NMRD) spectroscopies, ^1H nuclear Overhauser effect (NOE) of paramagnetic compounds and NMR of magnetically coupled dimers have been helpful in shedding light on the complex problem. Site-directed mutagenesis has provided the variety of derivatives necessary to chemists to relate the structure and function of molecules.

B. INVESTIGATION OF THE COPPER(II) SITE

Copper(II) is a good spectroscopic probe [63–65]. It is a d^9 metal ion with a ^2D ground state configuration. The ligand field splits this term into up to five levels. Most often, however, copper(II) gives rise to a single broad band in the visible region and does not allow the detection of the various transitions [66]. In the present case, in which copper is bound to a protein, circular dichroism (CD) spectroscopy can be of further help [67,68].

As will be shown in more detail, the electronic relaxation times of copper(II) in SOD are around 2×10^{-9} s. This long time allows detection of the EPR signal even at room temperature, with the copper hyperfine splitting resolved. The g values and the parallel hyperfine coupling values are very meaningful parameters [69,70]. ^1H and ^{14}N ENDOR and ESE measurements are also feasible [71–73]. Finally, water ^1H NMRD data provide information on the electronic correlation time τ_s, and on the presence of exchangeable water protons interacting with the paramagnetic centre [74–77]. Owing to the large τ_s value, the system is not suitable for NMR measurements. However, under fast exchange conditions and in the presence of excess ligand, NMR spectroscopy of ligand nuclei is possible and instructive. The ^1H NMR of the Cu_2Co_2 and Cu_2Ni_2 derivatives will be discussed in Section C.

(i) Electronic absorption and CD spectra

The absorption and CD spectra of native Cu_2Zn_2BeSOD are reported in Fig. 4(a) [78]. A shoulder at 24000 cm^{-1} and a very broad band at 14700 cm^{-1} appear in the electronic spectrum. The broad band at 14700 cm^{-1} is assigned to d–d transitions; by CD spectroscopy two transitions are observed at about 13000 and 16000–17000 cm^{-1}; a third transition has been postulated at about 19000 cm^{-1} [78]. The shoulder at 24000–25000 cm^{-1} was assigned to bridging imidazolato-to-copper ligand-to-metal charge transfer (LMCT) [78,79]. The band disappears in the zinc-depleted enzyme and is present in all derivatives in which zinc(II) is replaced by copper(II),

cobalt(II), cadmium(II) and mercury(II) [27]. This band is indicative of the presence of the imidazolato bridge in solution, and shows that an imidazolato bridge is present in all binuclear derivatives. An earlier proposal [80(a)] based on perturbed angular correlations of γ-rays that His-63 is not bridging in the Cu_2Cd_2SOD derivative has recently been corrected using the same technique [80(b)]. Near-UV absorption and CD spectra of Cu_2Zn_2BeSOD are reported in Fig. 4(b). Analysis of the difference absorption spectrum of native enzyme from apoenzyme allows detection of three very broad bands at about 40 000 cm^{-1} ($\epsilon = 3300\ M^{-1}\ cm^{-1}$), 35 000 cm^{-1} ($\epsilon = 1000\ M^{-1}\ cm^{-1}$) and 30 000 cm^{-1} ($\epsilon = 300\ M^{-1}\ cm^{-1}$). The CD spectra show the same bands with a decrease in band linewidth [78]. Zinc(II) complexes have absorption bands in the UV region only in the presence of ligands susceptible to oxidation; therefore the UV bands have been assigned to LMCT bands of copper. LMCT absorptions have been extensively studied, particularly in the field of copper(II) proteins [81]; assignment of the electronic transitions of SOD is supported by analysis of various imidazole and imidazole model complexes [79,81]. In the case of the zinc-depleted derivative the ellipticity of the LMCT bands is increased, while that of *d–d* transitions is decreased with respect to the native enzyme; this indicates that imidazoles are still coordinated to copper but the geometry has been

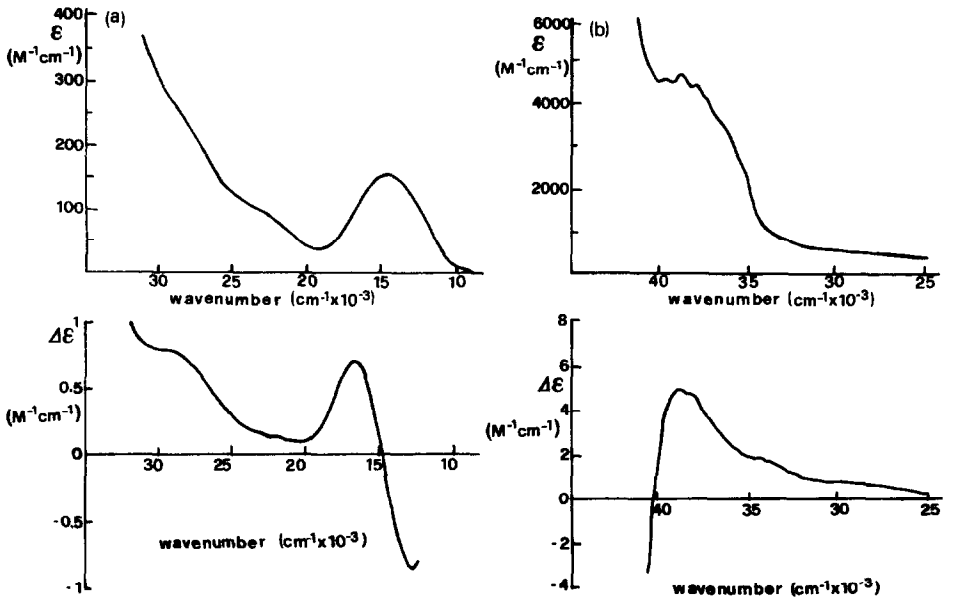

Fig. 4. Visible (a) and UV (b) electronic and CD spectra of BeSOD. The molar absorbances and differential molar absorbances are per copper site [78].

modified in the sense of a more regularly tetragonal coordination structure. The absence of the 24000–25000 cm^{-1} bands is consistent with the protonation of the imidazolate coordinated to copper(II) [78]. The electronic spectra are essentially pH independent in the pH range 4–10.5. At low pH (pK_a ca. 3) the bridging histidine is protonated on the nitrogen facing zinc [82].

(a) Electronic transitions in the anion derivatives

Table 3 shows the electronic transitions from the CD spectra of the copper chromophore in the presence of various anionic ligands [83]. In comparison with the non-inhibited spectra, the band assigned as the imidazolato-to-copper charge transfer band does not change its position much, indicating that the imidazolato bridge between the two metals is not changed. However, the energies of the *d–d* transitions reflect some changes in coordination geometry. The electronic spectra (not shown) display only one band in all cases; its energy, which can be taken as a rough average of the resolved CD bands, reflects the mean crystal field splitting between the e_g and t_{2g} orbitals in octahedral symmetry. The energy of this band is about the same as that of the non-ligated enzyme for the F^- and the NCS^- derivatives (14.7×10^3 cm^{-1}), increases with NCO^- and N_3^- (15.1×10^3 cm^{-1}) and reaches a value of 19.3×10^3 cm^{-1} in the CN^- derivative [84–86]. In the CD spectra (Table 3), two or three *d–d* transitions can be resolved [78,83]. Inspection of Table 3 reveals that NCS^-, which does not seem to perturb the electronic spectrum, has a detectable effect on the CD spectra. The splitting of the bands increases from native and F^- to NCS^- and NCO^- adducts, and then decreases from NCO^- to N_3^- and CN^-. Although a detailed assignment would require observation of all three bands in all cases, this observation could be taken as an indication of a progressive shift from a puckered (tetrahedrally distorted) square-planar to a more regular square-planar geometry.

TABLE 3

Electronic transitions from CD measurements on anion adducts of BeSOD [a]

Derivative	Transition energies ($\times 10^{-3}$ cm^{-1})				
Native		13.4		16.5	24
F^-		13.4		16.5	24
NCS^-		13.3		16.7	25
NCO^-	<13	15.1		19.4	25
N_3^-	14.3	18.5		> 20	24.7
CN^-			20.4		24.4

[a] Taken from ref. 83 and unpublished results from our laboratory.

TABLE 4

Energies of the electronic transitions of SOD isoenzymes and mutants from CD measurements [a]

Derivative	Transition energies ($\times 10^{-3}$ cm^{-1})						
YSOD	13.0	15.9	23.7	28.0	30.5	37.0	42.5
HeSOD [b]	13.4	16.5	25.3	29.3	33.0	40.4	42.9
HYSOD [c]	13.4	16.5	25.3	29.3	33.0	40.4	42.9
AS-HYSOD	13.4	16.5	25.3	29.3	33.0	40.4	42,9
Ile-143	13.7	16.5	25.3	29.4			
Lys-143	14.0	16.8	25.0	29.4			
AS Glu-143	14.3	16.9	25.3	30.3	33.9	40.8	42.5
Ile-137	14.3	17.6	25.2	28.5	33.7	41.0	42.8

[a] From ref. 58. The values are obtained through computer simulation of the spectra using gaussian line shapes. [b] Human erythrocyte SOD. [c] WT human SOD expressed in yeast.

(b) CD spectra of SOD isoenzymes and mutants

The electronic transitions detected through computer simulation of the CD spectra of various SOD isoenzymes and mutants are reported in Table 4 [58]. The derivatives are arranged in order of increasing *d–d* transition energies. It can be noted that HSOD is very similar to BeSOD, while YSOD has slightly lower *d–d* and LMCT energies. All the mutants show a progressive increase in tetragonality, the maximum being reached with the Ile-137 derivative [58,59].

(ii) EPR spectra

The EPR spectrum for the Cu_2Zn_2BeSOD isoenzyme is reported in Fig. 5 [38,47,87]; the spectra of all the characterized isoenzymes are highly anisotropic, as expected for a distorted CuN_4O chromophore [58,88]. Single-crystal measurements on the bovine isoenzyme provide the principal values of the g tensor (2.03, 2.09 and 2.26). The principal values of the A tensor are 52.5, 34.6 and 142×10^{-4} cm^{-1} [89].

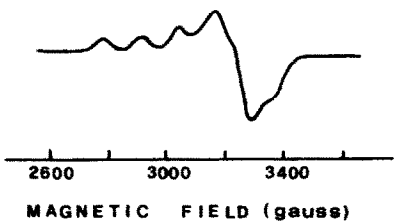

Fig. 5. X-band EPR spectrum of BeSOD at pH 6.1 and 303 K [86].

TABLE 5

EPR parameters [a] of BeSOD, its inhibitor derivatives and other isoenzymes and mutants

	$g_{\parallel}$	$g_{\perp}$ [a]	$A_{\parallel}$ ($\times 10^4$ cm^{-1})	Ref.
BeSOD [b]	2.26	2.07	141	38, 47
BeSOD + F^- [b]	2.26	2.07	143	85
BeSOD + NCS^- [b]	2.25	2.06	148	84
BeSOD + NCO^- [b]	2.26	2.05	158	85
BeSOD + N_3^- [b]	2.24	2.04	157	85
BeSOD + CN^- [c]	2.21	2.04	188	89
YSOD [b]	2.26	2.08	141	27
HeSOD [b]	2.26	2.07	140	88
HYSOD [d]	2.28	2.09	147	58
AS-HYSOD [d]	2.28	2.09	142	58
HYSOD – Lys-143 [d]	2.25	2.07	150	58
HYSOD – Ile-143 [d]	2.26	2.08	138	58
HYSOD – Glu-143 [d]	2.28	2.09	148	58
HYSOD – Ile-137 [d]	2.27	2.06	166	58

[a] All spectra except the spectrum of the cyanide derivative are assumed to be axial. Reported value for $g_{\perp}$ of BeSOD + CN^- has been obtained from single-crystal EPR [89], by considering the average value of g_x and g_y. [b] Data on liquid-nitrogen frozen solutions. [c] Single-crystal 77 K measurements. [d] Room temperature measurements.

Although the principal axes of the g tensor cannot be unequivocally settled, the z axis can be roughly described as normal to the N_4 plane. Superhyperfine splitting is observed in the cyanide derivative, which is consistent with three coordinated nitrogen atoms [89].

The EPR spectra of frozen solutions at 77 K are available for many anion derivatives, mostly at X band. The $A_{\parallel}$ and $g_{\parallel}$ parameters are easily read (Table 5). In the case of rhombic spectra, only an approximate $g_{\perp}$ value is reported. The EPR spectra of BeSOD, HeSOD and YSOD are very similar [27,38,47,86,88,90]. All the mutants show similar spectra although an increase in $A_{\parallel}$ is observed in parallel with the increase in energy of the optical d–d transitions [58,90]. In particular, Ile-137 has the largest $A_{\parallel}$ value, which would be expected to correspond to a less distorted chromophore [59].

Anions tend to give rise to more axial spectra. This is possibly due not to a real increase in symmetry, but to the formation of a CuN_3X plane with some minor axial perturbations [84,85]. Cyanide provides the largest $A_{\parallel}$ and the smallest $g_{\parallel}$ values, consistent with an essentially planar structure [86]. If a large $A_{\parallel}$ value is taken as an indication of a square-planar structure, N_3^- and NCO^- are next, followed by NCS^- and F^-. This is also the order of decreasing affinity of the anions for the enzyme [48,49].

(iii) ENDOR and ESE spectra

The ^{1}H and ^{14}N ENDOR spectra have been measured at 4.2 K for the bovine [91,92] and human [92] isoenzymes and for the bovine zinc-depleted [92], azide [92] and cyanide [91,92] derivatives. The ^{14}N ENDOR spectra show parallel hyperfine coupling values of about 39–40 MHz, with a quadrupolar splitting of the order of 1–1.5 MHz. The hyperfine values are typical of directly coordinated nitrogen atoms [93]. The low resolution has not allowed the separation of the signals due to the various nitrogen atoms. The ^{1}H ENDOR spectra in H_2O, recorded by saturating the lowest hyperfine split feature in the $g_{\|}$ region, i.e. when the external magnetic field is

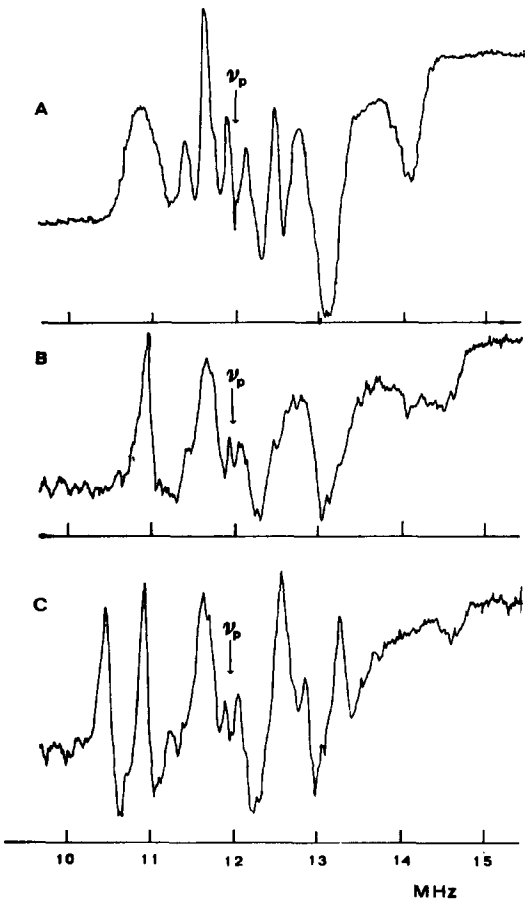

Fig. 6. ^{1}H ENDOR spectra for BeSOD (A), BeSOD + N_3^- (B), BeSOD + CN^- (C) in H_2O at about 10 K obtained upon irradiating the lowest field component of the hyperfine-split $g_{\|}$ feature [92].

along the molecular z axis, show about six different hyperfine couplings (Fig. 6) [92]. A larger number of signals is observed when other features of the EPR spectrum are saturated, i.e. when the magnetic field is not along a principal molecular axis. The spectra do not change when recorded in D_2O. This is rather surprising since there should be a coordinated water molecule in addition to the exchangeable NH protons of the coordinated histidine rings. It is possible that the other signals are due to histidine protons close to the coordinated metal.

The hyperfine coupling is given by a contact term and a dipolar term. The former can be estimated from the ^1H NMR spectra of the Cu_2Co_2 derivative [83] and the latter can be calculated, in the point-dipole approximation, with the formula

$$A_{(MHz)} = \frac{\mu_0}{4\pi} \sum_i \frac{g_e \mu_B g_n \mu_n \rho_i}{r_i^3} (3 \cos^2 \theta_i - 1) \qquad (2)$$

where ρ_i is the electron spin density at the ith ligand atom and θ_i is the angle formed by the vector of length r_i connecting the proton and the ith ligand atom with the direction of the magnetic field. The r_i values are known from the X-ray structure and the θ_i values can be evaluated in a frozen solution if the direction of the $g_{\|}$ axis with respect to the molecular frame is known. The comparison between the experimental and the calculated values has allowed the proposal of a tentative assignment of the ^1H ENDOR signals.

In the presence of azide the ^1H ENDOR spectra of both Cu_2Zn_2SOD and Cu_2E_2SOD do not show any appreciable change (Fig. 6B) [92]; despite this, there is agreement that azide does bind the metal. On the contrary, some changes occur in the presence of cyanide (Fig. 6C). The ENDOR data then suggest that the surroundings of the copper ion do not change substantially in the presence of anions. This has to be reconciled with data obtained from other spectroscopies.

From ESE spectroscopy measurements, ^{14}N hyperfine coupling constants mostly of about 4 MHz and some in the range 1.5–0.7 MHz have been obtained [94]. They represent the coupling between copper and the distal nitrogen of each bound histidine. The data allowed the authors to suggest that the bridging histidine is not detached upon anion binding, and in agreement with the ENDOR studies, no major changes are observed upon azide binding.

(iv) Water ^1H NMRD measurements

The measurements of water ^1H T_1^{-1} values of solutions containing a paramagnetic metalloprotein aim at obtaining information about the pres-

ence of water interacting with the metal ion [74–76]. Such measurements are obtained in a large range of magnetic fields, corresponding to proton Larmor frequencies between 0.01 and 50 MHz, and are called nuclear magnetic relaxation dispersion [95]. Water is often in fast exchange from the copper coordination sphere. Therefore the measured water ^1H T_1^{-1} values are due to the contribution of the bulk water, to the diamagnetic contribution of the protein and to the paramagnetic contribution of the interaction with the metal ion:

$$T_1^{-1} = T_{1\,\text{water}}^{-1} + T_{1\,\text{dia}}^{-1} + T_{1\text{p}}^{-1} \tag{3}$$

Further, still neglecting the effect of chemical exchange, $T_{1\text{p}}^{-1}$ is given by the product $f_{\text{M}}T_{1\text{M}}^{-1}$ where f_{M} is the molar fraction of water molecules interacting with the metal ion and $T_{1\text{M}}^{-1}$ is their relaxation rate. In turn, $T_{1\text{M}}^{-1}$ is proportional to the reciprocal of the sixth power of the distance of the proton from the metal ion, multiplied by a function of the correlation time and of the magnetic field.

The general theoretical framework was first described by Solomon in 1955 [96]. However, it has been shown that the experimental data could be interpreted only if the electronic spin $S = 1/2$ level is considered to be split upon interaction with the $I = 3/2$ nuclear magnetic moment of copper [97]:

$$T_{1\text{M}}^{-1} \propto E^2 \left[\int_{-1}^{1} C_{\text{s}}(A_{\parallel}, A_{\perp}, \omega_{\text{s}}, \theta, \beta, \tau_{\text{s}}) F_{\text{s}}(A_{\parallel}, A_{\perp}, \omega_{\text{s}}, \beta, \tau_{\text{s}}) \,\text{dcos}\,\beta \right.$$
$$\left. + \frac{\tau_{\text{s}}}{1 + \omega_{\text{I}}^2 \tau_{\text{s}}^2} - \int_{-1}^{1} C_{\text{I}}(A_{\parallel}, A_{\perp}, \omega_{\text{I}}, \theta, \beta, \tau_{\text{s}}) \,\text{dcos}\,\beta \right] \tag{4}$$

where E is the electron–proton dipolar interaction energy, $A_{\parallel}$ and $A_{\perp}$ are the principal components of the electron–copper nucleus hyperfine coupling tensor, assumed axial, β is the angle between the $A_{\parallel}$ direction and the external magnetic field, which varies with rotation, and θ is the angle between the $A_{\parallel}$ direction and the metal–proton vector, which is a characteristic of the system. C_{s}, F_{s} and C_{I} are functions of the above variables. The first term in square brackets formally corresponds to the ω_{s}-containing term of the Solomon [96] equation (see below), the second to the ω_{I} term. With this approach, Bertini et al. [97] succeeded in interpreting the water ^1H NMRD data of SOD [98] (Fig. 7) and obtained a Cu–O distance of 2.4 Å and an estimate of the electronic relaxation time of 2×10^{-9} s [97].

The Cu–O distance is similar to that obtained through extended X-ray absorption fine structure (EXAFS) spectroscopy [99]. The X-ray structure places this water molecule somewhat further away, i.e. at 2.8 Å [17]. It is possible that second-sphere effects simulate a shorter distance.

Water ^1H NMRD have also been measured in the presence of anions (Fig. 8) [100]. It appears that CN^- removes any water from the vicinity of

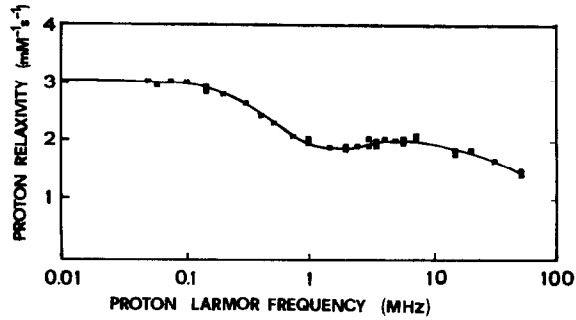

Fig. 7. Water ^{1}H NMRD data [98] at 298 K of solutions of BeSOD. The data are normalized to 1 mM copper ions. The curve is the best fitting to theory [97].

copper inside the cavity. Azide has a similar effect. Cyanate has some residual relaxivity. It is possible that a water molecule interacts with the anion and approaches copper at a non-bonding distance. In the case of thiocyanate, the decrease in relaxivity is even smaller. In the case of fluoride an increase in relaxivity, and therefore the presence of water interacting with the metal ion is observed [101]. It is possible that, together with fluoride and four histidines, a water molecule is present as a ligand further away in the coordination sphere in the sixth position or that a weaker water molecule interacts via hydrogen bonding with the coordinated fluoride.

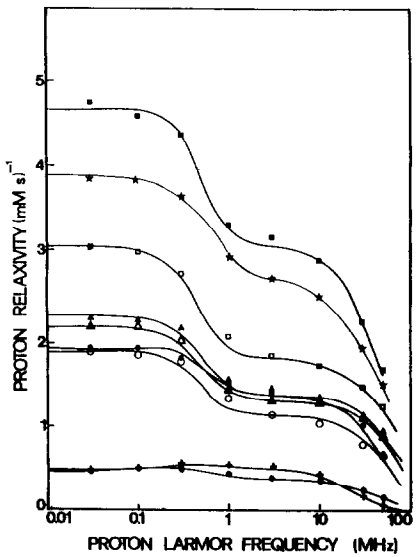

Fig. 8. Water ^{1}H NMRD data at 298 K of solutions of BeSOD and its anion derivatives: ■, $H_2PO_4^-$; ★, F^-; □, non-ligated BeSOD; ▲, 0.5 M NCS^-; △, 1 M NCS^-; ○, 2 M NCS^-; ●, NCO^-; +, CN^-; +, N_3^-. The data are normalized to 1 mM copper ions [100,101].

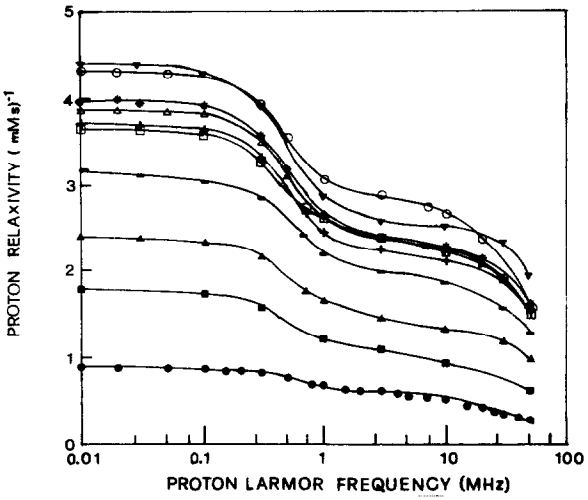

Fig. 9. ^{1}H NMRD profiles at 298 K of pH 5.5 solutions of BeSOD (▶), HYSOD-Ile-143 (○), AS-HEcSOD (△), HeSOD (+), HYSOD-Glu-143 (□), HYSOD (★), AS-HYSOD (■), YSOD (▲), HYSOD-Lys-143 (■) and HYSOD-Ile-137 (●) [90]. The values are obtained by subtracting from the water contribution and normalized to 1 mM copper concentration. The solid lines simply connect the experimental points.

Water ^{1}H NMRD data have been obtained for a series of mutants and isoenzymes [90] (Fig. 9). The T_{1p}^{-1} values around 4–10 MHz give a rough idea of the presence of water in the cavity sensing the paramagnetic metal ion. It appears that there are mutants with no water coordinated to copper (Ile-137) and some with water coordinated, as in the case of the bovine isoenzyme, for which the X-ray structure is known. As we shall see later, there is no relationship between activity and the presence of water near copper.

C. INVESTIGATION OF THE COPPER(II) SITE IN THE Cu_2Co_2 AND Cu_2Ni_2 DERIVATIVES

It is not possible to record ^{1}H NMR spectra of the native protein with the aim of detecting the protons of the groups coordinated at the copper(II) ions [74]. As we have anticipated, the electronic correlation time for the copper(II) ion is so large (2×10^{-9} s) [97] that it causes a dramatic broadening of the NMR signal of the protons sensing the unpaired electron. However, it is known that substitution of zinc(II) with cobalt(II) produces a derivative quite similar to the native protein and with essentially full activity [27].

The cobalt(II) ion in Cu_2Co_2SOD is high spin with $S = 3/2$ [102]. It is clear from the disappearance of the EPR signal at room temperature that

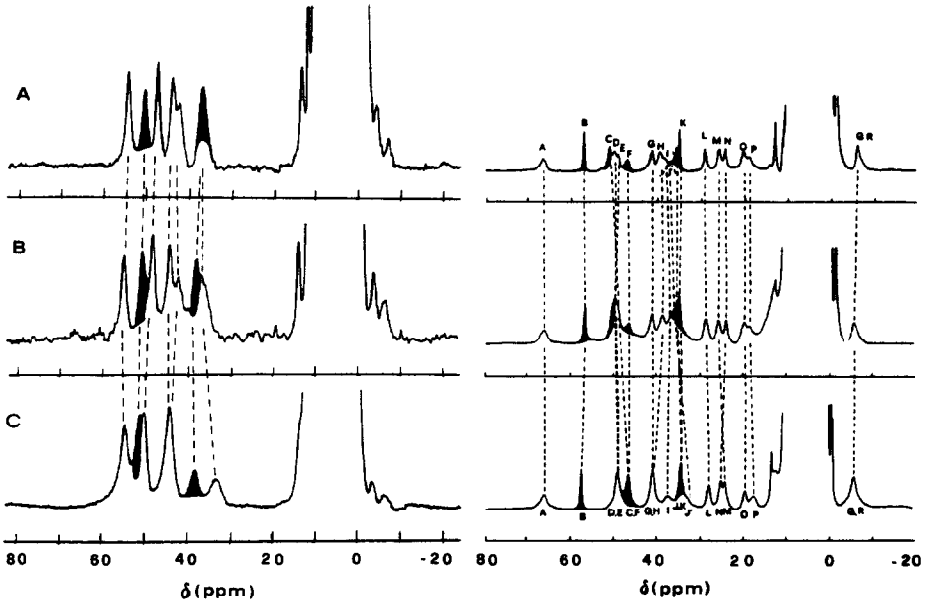

Fig. 10. 303 K ^{1}H NMR spectra of E_2Co_2SOD (left-hand side, at 200 MHz) and Cu_2Co_2SOD (right-hand side at 300 MHz) isoenzymes: A, BeSOD; B, HYSOD; C, YSOD [109]. The filled signals are due to exchangeable protons. Broken lines indicate correspondence among the signals of the three derivatives.

cobalt(II) is magnetically coupled with copper(II). We know that the electronic relaxation times of cobalt(II) in E_2Co_2SOD are about 4×10^{-12} s [103], i.e. they are short enough for the ^{1}H NMR proton lines of the coordinated histidines to be relatively sharp (Fig. 10, left-hand side). The occurrence of magnetic coupling provides the copper unpaired electron with new relaxation pathways through those of the unpaired electrons of cobalt [104,105]. The ^{1}H NMR spectra of Cu_2Co_2BeSOD show the signals of the protons of the histidines of both the copper and cobalt domain [83,103] (Fig. 10, right-hand side). The linewidths of the histidine protons of the copper domain are sharper than those of the histidine protons of the cobalt domain. This is because the linewidth depends on $S(S+1)$ which is $3/4$ for copper(II) and $15/4$ for cobalt(II). It has been shown by magnetic susceptibility measurements [106], that cobalt and copper in SOD are antiferromagnetically coupled with the ground state $S=1$ and the excited state $S=2$, separated by 33 cm^{-1}. The extent of this coupling ($J=16.5$ cm^{-1} for the Hamiltonian defined as $J\, S_1 \cdot S_2$) is larger than $\hbar\tau_{s(Co)}^{-1}$, which corresponds to about 1 cm^{-1} and leads one to expect that the electron relaxation time of copper approaches that of cobalt [107].

Recently, a Cu_2Ni_2SOD derivative was reported [29]. Its ^{1}H NMR signals are sharper than those of the analogous Cu_2Co_2 derivative (Fig. 11).

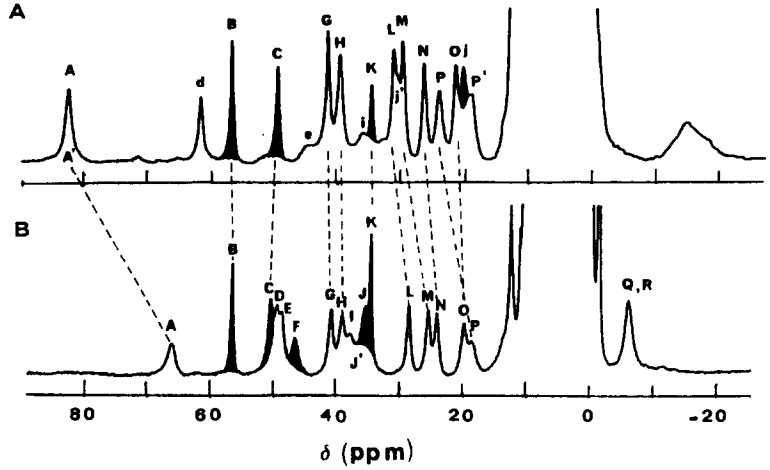

Fig. 11. 303 K and 300 MHz ^{1}H NMR spectra of Cu_2Ni_2BeSOD [29,108] (A) and Cu_2Co_2BeSOD [83,103] (B). The filled signals are due to exchangeable protons. The broken lines indicate correspondences among signals of the two derivatives for the copper domain.

This is due to the shorter electronic relaxation times of tetrahedral nickel(II) [74]. The assignment of the protons of the copper donors is performed by analogy with the spectra of the Cu_2Co_2 derivative [108].

(i) ^{1}H NMR spectra of Cu_2Co_2SOD

The ^{1}H NMR spectra of the bovine, human and yeast isoenzymes of the Cu_2Co_2SOD derivative are reported in Fig. 10, together with the spectra of the corresponding E_2Co_2SOD derivative [109]. The full assignment of the spectra has been puzzling. Firstly by recording the spectra in D_2O, it was possible to assign the histidine ring NH signals which are shown in black in Fig. 10 [83]. The rate of $^1H/^2H$ exchange depends on solvent accessibility of the histidine NHs, and the NHs of the copper domain are more accessible than those of the cobalt domain. Therefore we have assigned signals B, C and K as copper histidine NHs. Secondly, we have measured and analysed the T_1 values (Table 6). If the coupling between the proton and the unpaired electron(s) were dipolar, metal centred in nature, with the S manifold unsplit at zero magnetic field, the following equation would be expected to be valid [96,103,104,107]:

$$T_{1M}^{-1} = a\frac{2}{15}\left(\frac{\mu_0}{4\pi}\right)^2 \gamma_I^2 g_e^2 \mu_B^2 r^{-6} S(S+1) \times \left[\frac{6\tau_c}{1+(\omega_I+\omega_S)^2\tau_c^2} + \frac{3\tau_c}{1+\omega_I^2\tau_c^2} + \frac{\tau_c}{1+(\omega_I-\omega_S)^2\tau_c^2}\right] \quad (5)$$

TABLE 6

300 MHz ^{1}H NMR shift and T_1 values at 303 K for the isotropically shifted signals in the Cu_2Co_2BeSOD derivative [a]

Signal	δ (ppm)	T_1 (ms) [b]
A	66.2	1.1
B	56.5	4.1
C	50.3	[c]
D	49.4	3.1
E	48.8	3.1
F	46.7	2.4
G	40.6	2.8
H	39.0	1.7
I	37.4	1.4
J′	35.6	1.7
J	35.4	[c]
K	34.5	4.5
L	28.4	4.2
M	25.3	2.5
N	24.1	2.5
O	19.6	2.4
P	18.7	1.2
Q	−6.2	2.2
R	−6.2	2.2

[a] Taken from ref. 83. [b] Estimated errors are within ±15%. [c] Not measured because under a complex envelope.

where τ_c is the electronic relaxation time of either the cobalt or the copper ion, γ_I is the proton magnetogyric ratio, μ_B is the Bohr magneton, and the other symbols have the standard meaning or are defined in eqn. (4), and a is defined below. As pointed out for eqn. (4), the sets of constants in front of the parentheses are proportional to the square of the electron–nucleus coupling energy. Since the magnetic coupling causes two electronic levels to be occupied ($S = 1$ and 2) we have to sum the square of the coupling energy for the two levels. This gives two coefficients which are 7/8 for cobalt and 3/8 for copper [103,104,107]. These coefficients are indicated as a in eqn. (5). Therefore, we expect a large ratio between the T_1^{-1} values of the protons of the copper and cobalt domains if the τ_c values are similar; on the contrary we observe T_1 values in a very small range (Table 6). This has been semiquantitatively accounted for by assuming that the unpaired electron(s) is largely delocalized onto the histidine ligand [103]. A small fraction of unpaired spin density on a π orbital of the histidine may give rise to sizeable contributions to T_1^{-1} since the electron–nucleus distance is relatively small (ligand-centred effects [110]). If, for some reason, a proton of the copper

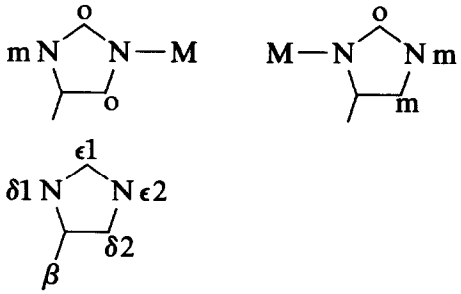

Scheme 1.

domain senses a larger ligand-centred effect it may have a larger T_1^{-1} value than a proton of the cobalt domain. The presence of ligand-centred effects is demonstrated by the ratio between T_1^{-1} of *meta*-like and *ortho*-like protons of a histidine ring bound to the same metal ion. *Ortho*-like and *meta*-like protons are defined with respect to the coordinating nitrogen as in Scheme 1.

The ratio between the T_1 values of the *ortho* and *meta* protons should be about 1 : 22. In the presence of ligand centred effects, spin delocalization quenches such a ratio. With these serious limitations, we have tentatively assigned the signal (among the non-exchangeable protons) with largest T_1 (signal L) to the only *meta*-like proton of the copper domain (Hδ2 of His-46; for the labelling of the ring protons, see Scheme 1). It was later shown that such a proton gives rise to signal G [111]. Among the other signals, the signals with the largest T_1 values were assigned to the *meta*-like protons of the cobalt domain (signals D and E). All other signals apart from I and J′ are assigned to *ortho*-like protons of the copper domain. Signal A has the largest shift and the smallest T_1; it is assigned to a proton of the bridging histidine (His-63).

The linewidth has been measured between 60 and 400 MHz. At low magnetic fields (i.e. corresponding to 60–200 MHz proton Larmor frequency) the dipolar coupling model should hold [96,103,104,107]:

$$T_{2M}^{-1} = a\frac{1}{15}\left(\frac{\mu_0}{4\pi}\right)^2 \gamma_I^2 g_e^2 \mu_B^2 r^{-6} S(S+1)\left[4\tau_c + \frac{6\tau_c}{1+(\omega_I+\omega_S)^2\tau_c^2} + \frac{6\tau_c}{1+\omega_S^2\tau_c^2} + \frac{\tau_c}{1+(\omega_I-\omega_S)^2\tau_c^2} + \frac{3\tau_c}{1+\omega_I^2\tau_c^2}\right] \quad (6)$$

where all the symbols have the same meaning as in eqn. (5); a is the coefficient due to magnetic coupling and equals 3/8 for copper and 7/8 for

TABLE 7

Linewidth (Hz) at 300 K for the ^{1}H NMR signals of Cu_2Co_2BeSOD at various magnetic fields [a]

Signal	Proton resonance frequency (MHz) [b]				
	60	90	200	300	400
A	230	220	360	440	512
B	115	110	130	115	124
C	150	120	170	230	310
D	180	170	200	295	395
E	120	170	195	295	395
F	200	190	270	460	540
G	130	130	160	240	284
H	220	260	240	320	360
I	380	290	395	520	930
J′	480	280	410	550	930
J	280	160	275	350	474
K	160	80	80	95	117
L	190	106	160	200	255
M	160	115	210	240	280
N	160	120	205	235	280
O	250	190	250	280	340
P	330	250	340	480	530

[a] Taken from ref. 103. [b] The corresponding magnetic fields are 1.41, 2.11, 4.70, 7.05 and 9.40 T.

cobalt, as in the case of T_1. The equation holds if the resulting proton senses only one metal with its a and τ_c. At large magnetic fields, another contribution (Curie relaxation) is expected to be sizeable and eventually dominant [112,113]:

$$T_{2M}^{-1} = a\frac{1}{5}\left(\frac{\mu_0}{4\pi}\right)^2 \omega_I^2 g_e^4 \mu_B^4 r^{-6} S^2 (S+1)^2 (3kT)^{-2}\left[4\tau_r + \frac{3\tau_r}{1+\omega_I^2\tau_r^2}\right] \qquad (7)$$

where all the symbols have the usual meaning.

Protons close to the unpaired electrons should have increasing linewidths above 200 MHz, and the slope should be dependent on the distance. The data in Table 7 have been analysed in order to classify tentatively the protons of the copper domain (slope dependent on $S = 1/2$), those of the cobalt domain (slope dependent on $S = 3/2$) and, within each domain, to distinguish between the *ortho*-like and *meta*-like protons [103]. The agreement of the experimental data with the final assignment is rather approximate. Finally, we produced an HSOD derivative, expressed from *E. coli* with histidines deuterated at position $\epsilon 1$ [114]. Signals H, M and O disap-

peared from the spectrum of Fig. 10, thus providing unambiguous assignments for these signals.

(ii) ^1H NOE measurements on Cu_2Co_2SOD

When an NMR signal is saturated, another signal may experience a variation in intensity; this is termed the nuclear Overhauser effect (NOE). The NOE, η_{ij}, measured at steady state for two isolated nuclear spins at distance r, dipolarly coupled, when i is irradiated and j is observed, is given by [115]

$$\eta_{ij} = \sigma_{ij}/\rho_j \tag{8}$$

where σ_{ij} is the cross-relaxation and ρ_j is the selective T_1^{-1} of the observed signal. The selective T_1, measured under selective excitation of a signal, depends on the structural and dynamic parameters as in eqn. (5). In the case of paramagnetic molecules it is dominated by the dipolar interaction with the unpaired electrons and therefore it depends on the inverse of the sixth power of the nucleus–unpaired electron distance. The cross-relaxation term, σ_{ij}, is due to the dipolar interaction between the two nuclear spins i and j and therefore it depends on the inverse of the sixth power of their internuclear distance. Thus, for two nuclei of the same species we have

$$\sigma_{ij} = \frac{1}{10}\left(\frac{\mu_0}{4\pi}\right)^2 \hbar^2\gamma^4 r_{ij}^{-6}\left[\frac{6\tau_c}{1+\omega_I^2\tau_c^2} - \tau_c\right] \tag{9}$$

where the correlation time τ_c is the rotational (or spin reciprocal reorientation) correlation time.

The fast proton relaxation in paramagnetic systems in a way simplifies the measurements, as only first-order NOEs are usually observed; however, the NOEs are quite small owing to the large ρ_j values. Only the recent advances in NMR technology have allowed some researchers to exploit NOEs of the order of 1% in a reliable and valuable way. La Mar and coworkers at the University of California at Davis have pioneered this field [116–118] and made NOE studies in paramagnetic molecules reliable.

^1H NOE measurements have been performed in Cu_2Co_2SOD and effects have been measured among protons of the copper domain only, because the T_1 values are longer than those in the cobalt domain [111]. It has been possible to detect NOEs between vicinal protons in the same histidine ring. By saturating the signal due to the NH proton of His-46, NOEs on two signals are expected and observed. In Fig. 12 the difference spectra from the NOE experiments are shown, and in Table 8 the NOE values are reported. NOEs have been observed between protons of different histidines, and with

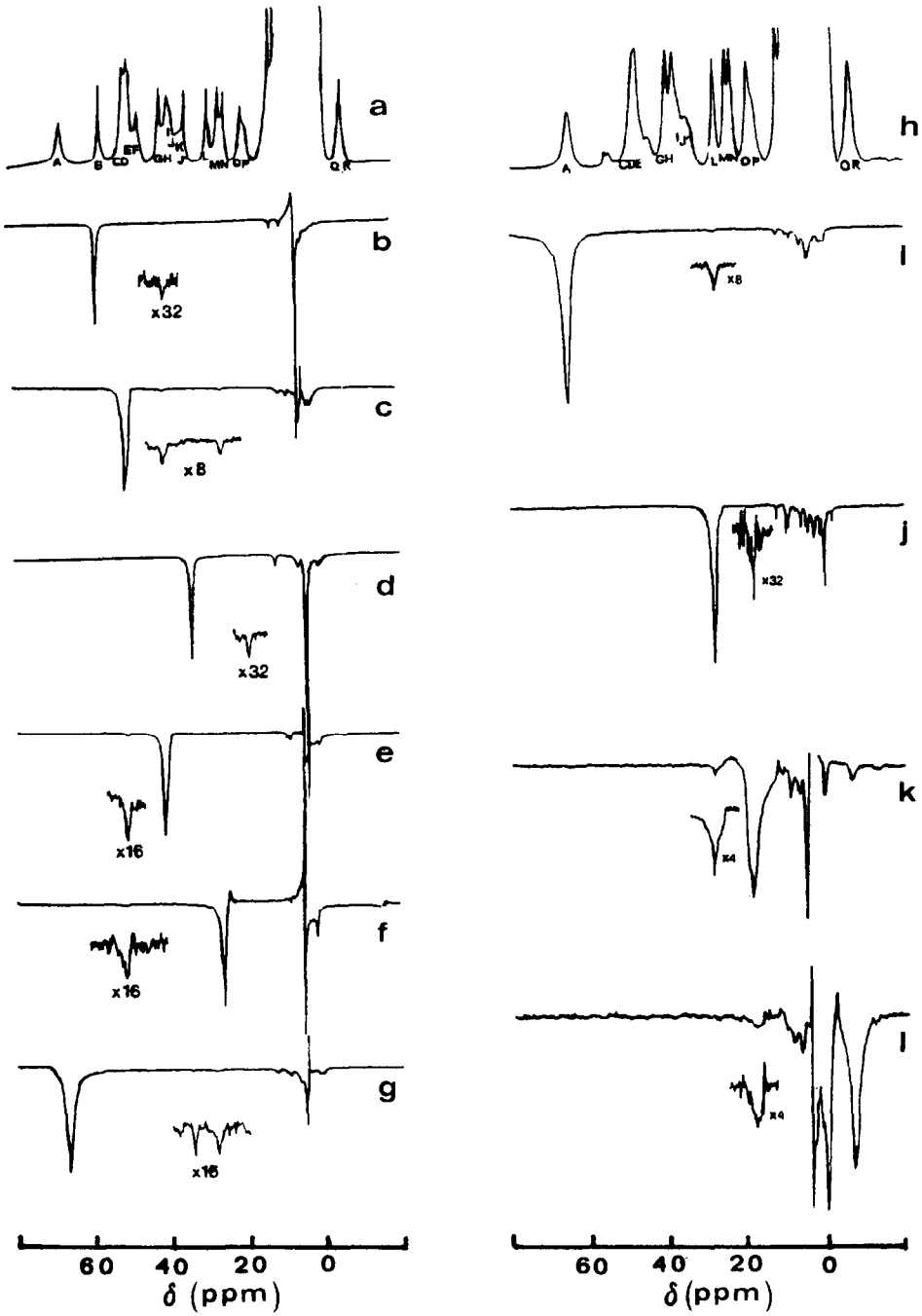

Fig. 12. ^1H NMR spectra and NOE difference spectra of Cu_2Co_2SOD at 300 K in H_2O (left-hand side) and D_2O (right-hand side) [111]. Left-hand side: a, reference spectrum; traces b–g show NOE difference spectra obtained by saturating signals B (b), C (c), K (d), G (e), M (f) and A (g) respectively. Right-hand side: h, reference spectrum; traces i–l show NOE difference spectra obtained by saturating signals A (1), L (j), P (k) and Q (l), respectively. All the spectra have been recorded at 200 MHz except b and j, which were recorded at 300 MHz and 500 MHz respectively.

TABLE 8

Observed nuclear Overhauser enhancements [a] between isotropically shifted signals in Cu_2Co_2BeSOD

Saturated peaks	Observed peaks							
	K	L	H	G	O	M	P	Q, R
A	0.8	1.1 0.4 [e]			0.4			0.2
B			1.3					
C				1.8 2.2 [b]		1.2 2.8 [d]		
K					0.8			
L							1.7 7.0 [c]	0.7
P								11

[a] Taken from ref. 111. The data were recorded at 200 MHz and 300 K and are reported as percentage decreases in signal intensity. They were obtained by simulation of the difference spectra. The estimated error on these data is ±30%. [b] NOE observing signal C by saturating G. [c] NOE observing signal L by saturating P. [d] NOE observing signal C by saturating M. [e] NOE observing A by saturating L.

the help of selective histidine deuteration a final assignment is obtained as reported in Table 9. NOEs have also been detected between the geminal protons of the β-CH_2 group of Asp-83 of the cobalt domain on account of their short distance apart [114]. Finally, NOEs have been observed between protons of the coordinated histidines and protons in the diamagnetic part of the spectrum. These data provide important information which is being studied in order to explore the protein at a larger distance from the metal ions.

It should be noted that the shifts of the protons of the cobalt domain overlap those of the protons of the copper domain, probably on account of the strong ligand-centred effects. The shifts of His-48 protons are the smallest as a result of either the electronic property of copper (i.e. the unpaired electron resides in an orbital orthogonal to the Cu–N bond of His-48) or a larger Cu–N bond distance.

(iii) Reaction with anions

F^-, NCS^-, NCO^- and N_3^- bind copper(II) in SOD [46–53] and the exchange between free and bound anion is fast on the NMR time scale.

TABLE 9

300 MHz ^{1}H NMR shift and T_1 values at 303 K for the isotropically shifted signals in the Cu_2Co_2SOD derivative together with their assignment

Signal	δ (ppm)	T_1 (ms) [a]	Assignment
A	66.2	1.1	His-63 Hδ2 [b]
B	56.5	4.1	His-120 Hδ1 [b]
C	50.3		His-46 Hϵ2 [b]
D	49.4	3.1	His-80 Hδ2
E	48.8	3.1	His-71 Hδ2
F	46.7		His-80 Hϵ2 (His-71 Hϵ2) [c]
G	40.6	2.8	His-46 Hδ2 [b]
H	39.0	1.7	His-120 Hϵ1 [b]
I	37.4	1.4	Asp-83 Hβ1 (Asp-83 Hβ2) [c]
J′	35.6	1.6	Asp-83 Hβ2 (Asp-83 Hβ1) [c]
J	35.4	[d]	His-71 Hϵ2 (His-80 Hϵ2) [c]
K	34.5	4.5	His-48 Hδ1 [b]
L	28.4	4.2	His-48 Hδ2 [b]
M	25.3	2.5	His-46 Hϵ1 [b]
N	24.1	2.5	His-120 Hδ2 [b]
O	19.6	2.4	His-48 Hϵ1 [b]
P	18.7	1.2	His-46 Hβ1 [b]
Q	−6.2	2.2	His-71 Hβ2 [b]
R	−6.2	2.2	His-46 Hβ2 [b]

[a] Estimated errors are within 15%. [b] Ref. 111. [c] Refs. 103 and 114.

Therefore it is easy to follow the variation of the shifts as a function of anion concentration [83,101,109] and to make the assignment of the adducts. From titration with these anions it is possible to determine the constant for the reaction

$$\text{SOD} + \text{Anion} \rightleftharpoons \text{SOD} \cdot \text{Anion} \qquad (10)$$

Such constants are determined in the absence of constant ionic strength and therefore they may differ from estimations under different experimental conditions.

In the case of the CN^- derivative, the exchange between free and bound anion is slow [100,119]; therefore upon addition of CN^- the spectrum of Cu_2Co_2SOD disappears, whereas that of the cyanide adduct increases in intensity. The assignment of the latter has been made through saturation transfer and using the deuterium-labelled derivative. In this way all the signals have been unequivocally assigned (Fig. 13).

From the spectra of the anion adducts (Table 10) it appears that all the anions cause a decrease in the shifts of His-48 protons (signals L, K and O) though to different extents: cyanide quenches the isotropic shifts completely,

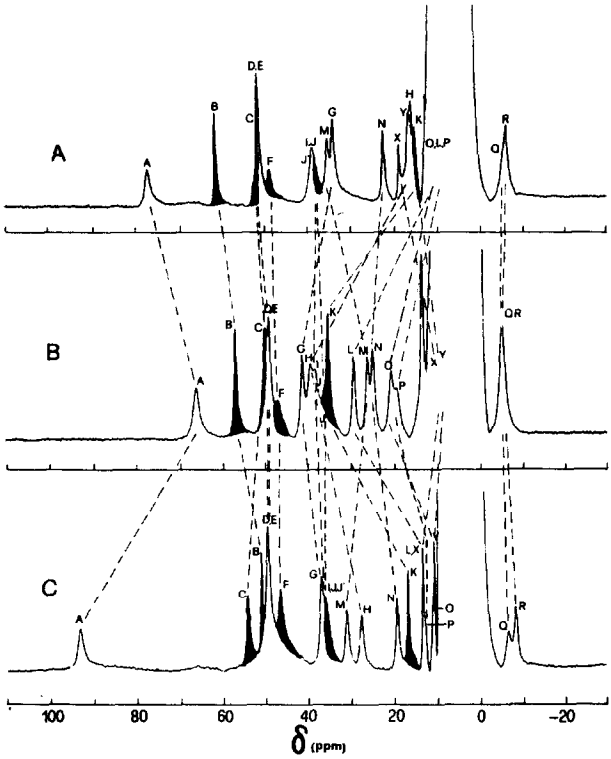

Fig. 13. 200 MHz ^{1}H NMR spectra of Cu_2Co_2BeSOD (B) and its cyanide (A) and azide (C) derivatives at 303 K. The samples contain about 1 mM enzyme in 50 mM Hepes buffer at pH 7.5. The filled signals disappear when the spectra are recorded in D_2O. The broken lines connect signals due to the same proton in the three derivatives. X and Y indicate protons which are unresolved in the diamagnetic region of the spectrum of Cu_2Co_2BeSOD (B) and move downfield upon addition of cyanide or azide [100,119].

followed, in order, by N_3^-, NCO^-, NCS^- and F^-. Other effects are present on other signals. The decrease in shift indicates that the unpaired spin density or spin delocalization decreases: the obvious consequence is that His-48 is removed from coordination upon CN^- or N_3^- binding. Another complicated explanation may arise from a change of molecular axes which could place the unpaired electron more and more orthogonal to His-48. Which of the two effects is dominant is still an open question. A reasonable model would be that anions bind at the site of the semicoordinated water. With strong donors, the basal *xy* plane would be formed by the anion donor and the other three histidines (Fig. 14). The copper ion could move towards the plane of the histidines. The Cu–N–His-48 distance would increase, possibly also as a result of a movement of the histidine.

TABLE 10

^{1}H NMR parameters for Cu_2Co_2BeSOD and its anion adducts at 303 K

Signal	Shift (ppm)				
	$+CN^-$ [a]	$+N_3^-$ [b]	$+NCO^-$ [c]	$+NCS^-$ [d]	Cu_2Co_2BeSOD
A	76.6	95.1	76.5	70.6	66.2
B	60.2	51.2	54.1	55.9	56.5
C	51.1	55.0	54.9	48.6 [e]	50.3
D	50.1 [e]	49.7	49.4	48.6 [e]	49.4
E	50.1 [e]	50.1	49.5	48.6 [e]	48.8
F	47.2	46.9	46.7	48.6 [e]	46.7
G	32.1	37.3	38.5	39.8	40.6
H	14.2	27.3	26.5	33.1	39.0
I	37.3 [e]	36.3	36.4	35.6 [e]	37.4
J′	37.3 [e]	35.7 [e]	36.7 [e]	35.6 [e]	35.6
J	37.3 [e]	35.7 [e]	36.7 [e]	35.6 [e]	35.4
K	13.0	15.9	19.8	30.2	34.5
L	9.1	12.5	15.6	24.9	28.4
M	33.7	31.4	32.0	27.1	25.3
N	20.4	18.9	19.8	22.6	24.1
O	<11	10.5	14.3	16.8 [e]	19.6
P	<11	11.6	13.0	16.8 [e]	18.7
Q	−8.7 [e]	−9.2	−7.7	−6.3 [e]	−6.2 [e]
R	−8.7 [e]	−7.4	−8.1	−6.3 [e]	−6.2 [e]

[a] Spectrum recorded at 200 MHz. Taken from ref. 119. [b] Titration performed at 300 MHz. From refs. 83 and 109. [c] Titration performed at 200 MHz. Unpublished results from this laboratory. [d] Titration performed at 60 MHz. Taken from ref. 83. [e] Signals unresolved.

At the other extreme, a weak ligand such as F^- displaces water but changes the molecular axes and the structure of the chromophore only slightly, with little consequence on the spectral parameters. The donor strength of the ligand, as expected from the spectrochemical series [66], is consistent with the order of the affinity of the ligands for the enzyme. In Fig. 15 the shift of signal L of His-48 vs. the affinity constant is reported. It is shown [119] that the larger the affinity constant of the ligand, the smaller the shift of signal L of His-48.

D. INFERENCES ON THE MECHANISM

It should be noted that the affinity constants of anions for the various mutants in the 143 position follow somewhat the pattern of catalytic activity (Table 11) [59–61]. This supports the idea that O_2^- is attracted inside the cavity with the same affinity pattern as the other anions, and that differences in activity depend on the different thermodynamic affinities for the

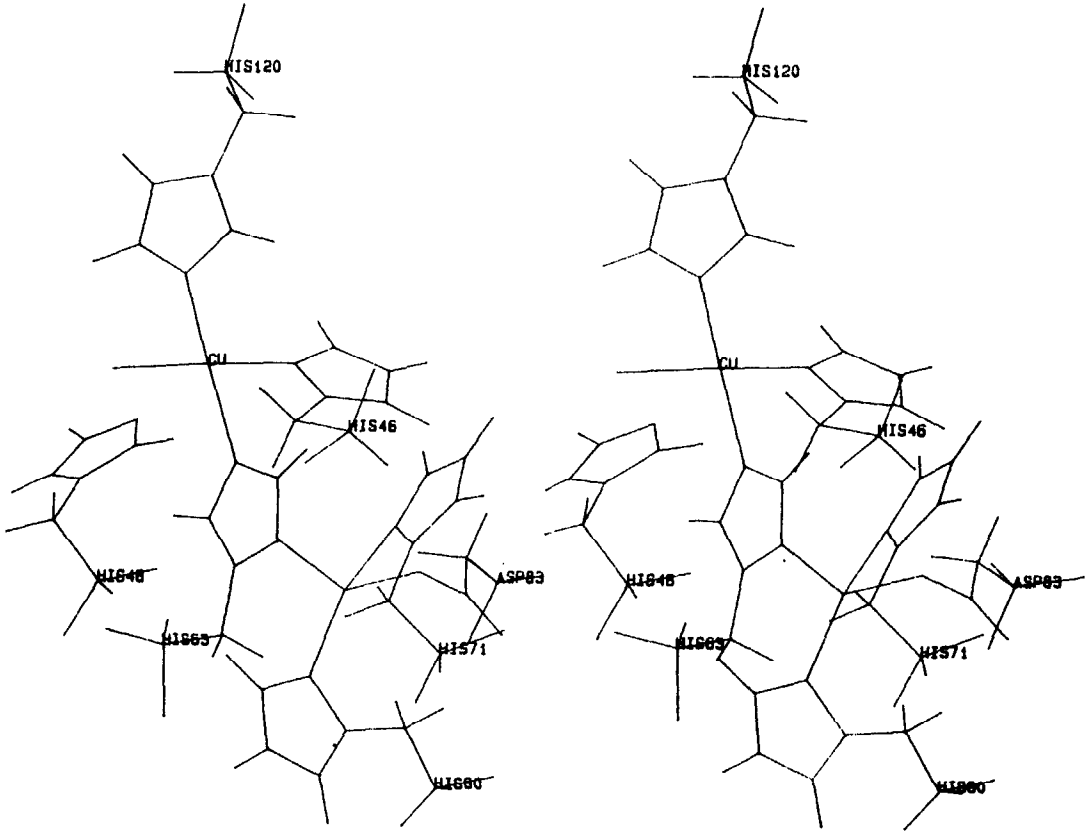

Fig. 14. Proposed structure of the adduct of SOD with strong binding ligands such as N_3^- or CN^-. The copper ion is in a regular square plane formed by the anion, His-120, His-48 and His-63. His-46 is thus substantially removed from coordination.

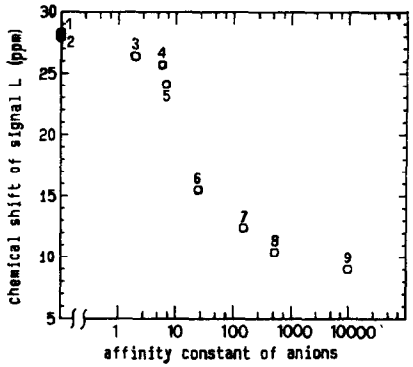

Fig. 15. Chemical shift of the L signal in several anionic adducts of different Cu_2Co_2SOD isoenzymes as a function of the affinity constant of the anion: Cu_2Co_2BeSOD–F^- (3); Cu_2Co_2YSOD–F^- (4); Cu_2Co_2BeSOD–NCS^- (5); Cu_2Co_2BeSOD–NCO^- (6); Cu_2Co_2BeSOD–N_3^- (7); Cu_2Co_2YSOD–N_3^- (8); Cu_2Co_2BeSOD–CN^- (9). For this adduct a lower limit of 10^4 for the stability constant has been considered. For comparison purposes the isotropic shifts in the pure Cu_2Co_2BeSOD (1) and Cu_2Co_2YSOD (2) isoenzymes are shown [119].

enzyme. The ^1H NMR spectra of the Cu_2Co_2 derivatives with N_3^- are all very similar to each other, as they are also without N_3^-. The difference in affinity of N_3^- for the derivatives must depend on the electrostatic properties of the cavity rather than on different structural properties [17,19]. We take this conclusion as evidence that the superoxide anion enters the cavity and probably interacts with Arg-143 when present. Malinowski and Fridovich [120] had shown that reaction of phenylglyoxal with Arg-143 provides an inactive derivative which displays a decrease in affinity for anions [121]. We had proved that phosphate interacts with Arg-143 [122] even though the inhibitory action of the anion has been questioned [123,124]. It is possible that Glu-133 and Lys-136 provide an electrostatic potential to guide super-

TABLE 11

Comparison between catalytic activity and azide binding constant for WT (Arg-143) and mutants at the 143 position [a]

Derivative	Activity (%)	N_3^- binding constant	
		(M^{-1})	(%)
Arg-143 (WT)	100	154	100
Lys-143	43	63	41
Ile-143	11	16	10
Glu-143	1	6	4

[a] Taken from ref. 61.

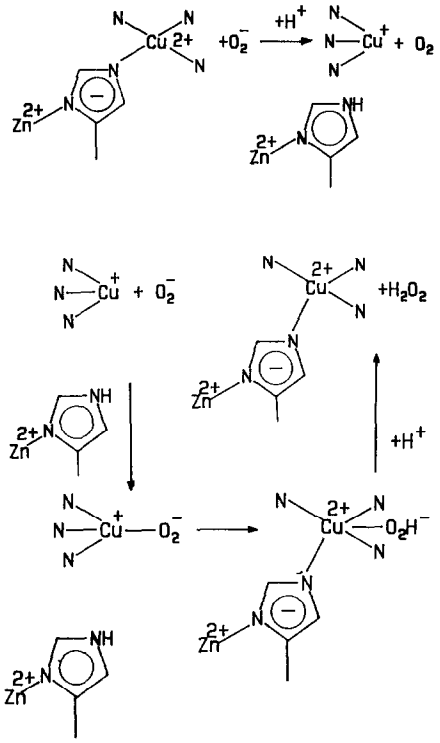

Fig. 16. Possible steps in the catalytic cycle. In the first step, O_2^- reduces the copper(II) ion; the bridge with His-63 is broken and the Nε2 nitrogen is protonated. Then a second superoxide ion binds copper(I), causing His-63 to coordinate again to the metal, which is reoxidized. Addition of a further proton liberates H_2O_2.

oxide inside the cavity [17]. Besides Arg-143, copper(II) should attract the anion. At this point the reduction of copper occurs (Fig. 16). The presence of water close to copper is not essential for the mechanism, as a derivative such as Glu-143 is inactive and has water whereas Ile-137 is active and has no water sensing copper [90]. The electron transfer may occur through direct coordination or through electron jump at a short O_2^-–Cu distance [125]. The reduced enzyme has no histidinato bridge [126–128]. His-63 is protonated in the pH range 5–10. The ^1H NMR spectra of $Cu_2^ICo_2SOD$ show evidence that three histidines are coordinated to cobalt with three NH protons at pH 5.5. The position of the signals does not change up to pH 10.5. At pH around neutrality, two NH signals disappear because of fast exchange with bulk water [129].

The NH proton of His-63 may be important for the second step of the reaction [130–133] when two protons are needed to produce hydrogen peroxide. However, the turnover is so fast that protonation and deprotona-

tion of His-63 may not occur and the protons may come from bulk water as pointed out by Fee and Bull [15].

The product (H_2O_2), if added in slight excess, is known to inhibit the enzyme activity [134–137]. Probably it reduces copper(II) to copper(I) which is reoxidized by atmospheric oxygen. During the reaction some radicals may be formed which react with the protein. Also the electronic properties of copper are changed [134,138–140]. It is suggested that the reaction is not specific at a site but is random [136,141,142].

Inactivation by H_2O_2 has also been followed for the mutants on the 143 position, with the suggestion that the enzymatic mechanism for HSOD Ile-143 is different [143].

REFERENCES

1 T. Mann and D. Keilin, Proc. R. Soc. (London), Ser. B, 126 (1938) 303.
2 R.J. Carrico and H.F. Deutsch, J. Biol. Chem., 245 (1970) 723.
3 J.M. McCord and I. Fridovich, J. Biol. Chem., 244 (1969) 6049.
4 I. Fridovich, Adv. Enzymol., 41 (1974) 35.
5 I. Fridovich, Adv. Enzymol. Relat. Areas Mol. Biol., 58 (1987) 61.
6 J.A. Fee, in H. Sigel (Ed.), Metal Ions in Biological Systems, Marcel Dekker, New York, Vol. 13, 1981, pp. 259–298; Trends Biochem. Sci., 7 (1982) 84.
7 G. Rotilio, L. Morpurgo, L. Calabrese, A. Finazzi-Agro and B. Mondovì, in B. Pullman and N. Goldblum (Eds.), Metal–Ligand Interactions in Organic Chemistry and Biochemistry, Part 1, Reidel, Dordrecht, 1977, p. 243.
8 A. Gaertner and U. Weser, Top. Curr. Chem., 132 (1986) 1.
9 J.S. Valentine and M.W. Pantoliano, in T.G. Spiro (Ed.), Copper Proteins, Vol. 3, Wiley, New York, 1981, Chapter 8, p. 291.
10 M.W. Parker, M.E. Schinina, F. Bossa and J.V. Bannister, Inorg. Chim. Acta, 91 (1984) 307.
11 D.O. Natvig, K. Imlay, D. Touati and R.A. Hallewell, J. Biol. Chem., 262 (1987) 14697.
12 D.T. Sawyer and J.S. Valentine, Acc. Chem. Res., 14 (1981) 393.
13 R.A. Hallewell, G.I. Bell, M.M. Stempien, E.D. Getzoff and J.A. Tainer, Proteins, 5 (1989) 322.
14 H. Gampp and A.D. Zuberbuehler, in H. Sigel (Ed.), Metal Ions in Biological Systems, Vol. 12, Marcel Dekker, New York, 1981, p. 133.
15 J.A. Fee and C. Bull, J. Biol. Chem., 261 (1986) 13000.
16 J.A. Tainer, E.D. Getzoff, K.M. Beem, J.S. Richardson and D.C. Richardson, J. Mol. Biol., 160 (1982) 181.
17 J A. Tainer, E.D. Getzoff, J.S. Richardson and D.C. Richardson, Nature (London), 306 (1983) 284.
18 E.D. Getzoff, J.A. Tainer, P.K. Weiner, P.A. Kollmann, J.S. Richardson and D.C. Richardson, Nature (London), 306 (1983) 287.
19 I. Klapper, R. Hagstrom, R. Fine, K. Sharp and B. Honig, Proteins, 1 (1986) 47.
20 E. Argese, A. Rigo, P. Viglino, E. Orsega, F. Marmocchi, D. Cocco and G. Rotilio, Biochim. Biophys. Acta, 787 (1984) 205.
21 H.M. Steinman, V.R. Naik, J.L. Abernethy and R.L. Hill, J. Biol. Chem., 249 (1974) 7326.

22 J.R. Jabusch, D.L. Farb, D.A. Kerschensteiner and H.F. Deutsch, Biochemistry, 19 (1980) 2310.
23 J.T. Johansen, C. Overballe-Petersen, B. Martin, V. Hasemann and I. Svendsen, Carlsberg Res. Commun., 44 (1979) 201.
24 M.W. Parker, F. Bossa, D. Barra, W.H. Bannister and J.V. Bannister, in G. Rotilio (Ed.), Superoxide and Superoxide Dismutase in Chemistry, Biology and Medicine, Elsevier, Amsterdam, 1986, p. 237.
25 J.V. Bannister, W.H. Bannister and E. Wood, Eur. J. Biochem., 18 (1971) 178.
26 U. Weser, G. Barth, C. Djerassi, H.-J. Hartmann, P. Krauss, G. Voelcker, W. Voelter and W. Voetsch, Biochim. Biophys. Acta, 278 (1972) 28.
27 K.M. Beem, W.E. Rich and K.V. Rajagopalan, J. Biol. Chem., 249 (1974) 7298.
28 J.S. Valentine, M.W. Pantoliano, P.J. McDonnell, A.R. Burger and S.J. Lippard, Proc. Natl. Acad. Sci. U.S.A., 76 (1979) 4245.
29 L.-J. Ming and J.S. Valentine, J. Am. Chem. Soc., 109 (1987) 4426.
30 J.A. Fee and R.G. Briggs, Biochim. Biophys. Acta, 400 (1975) 439.
31 S.J. Lippard, A.R. Burger, K. Ugurbil, M.W. Pantoliano and J.S. Valentine, Biochemistry, 16 (1977) 1136.
32 J.A. Fee, J. Biol. Chem., 248 (1973) 4229.
33 A.E. Cass, A. Galdes, H.A.O. Hill, C.E. McCleland and C.B. Storm, FEBS Lett., 94 (1978) 311.
34 D.B. Bailey, P.D. Ellis and J.A. Fee, Biochemistry, 19 (1980) 591.
35 L. Calabrese, D. Cocco and A. Desideri, FEBS Lett., 106 (1979) 142.
36 A.E.G. Cass, H.A.O. Hill, J.V. Bannister and W.H. Bannister, Biochem. J., 177 (1979) 477.
37 L.-J. Ming, Ph.D. Dissertation, U.C.L.A., 1988.
38 G. Rotilio, L. Calabrese, F. Bossa, D. Barra, A. Finazzi Agro and B. Mondovì, Biochemistry, 11 (1972) 2182.
39 K.M. Beem, D.C. Richardson and K.V. Rajagopalan, Biochemistry, 16 (1977) 1930.
40 L. Banci, I. Bertini, C. Luchinat, R. Monnanni, A. Scozzafava and B. Salvato, Gazz. Chim. Ital., 116 (1986) 51.
41 L. Banci, I. Bertini, C. Luchinat, R. Monnanni and A. Scozzafava, Inorg. Chem., 26 (1987) 153.
42 D. Klug-Roth, I. Fridovich and J. Rabani, J. Am. Chem. Soc., 95 (1973) 2782.
43 E.M. Fielden, P.B. Roberts, R.C. Bray, D.J. Loewe, C.H. Mautner, G. Rotilio and L. Calabrese, Biochem. J., 139 (1974) 49.
44 P. Viglino, A. Rigo, L. Calabrese, D. Cocco and G. Rotilio, Biochem. Biophys. Res. Commun., 100 (1981) 125.
45 J.A. Roe, A. Butler, D.M. Scholler, J.S. Valentine, L. Marky and K.J. Breslauer, Biochemistry, 27 (1988) 950, and references cited therein.
46 G. Rotilio, A. Finazzi Agro, L. Calabrese, F. Bossa, P. Guerrieri and B. Mondovì, Biochemistry, 10 (1971) 616.
47 J.A. Fee and B.P. Gaber, J. Biol. Chem., 247 (1972) 60.
48 A. Rigo, R. Stevanato and P. Viglino, Biochem. Biophys. Res. Commun., 79 (1977) 776.
49 A. Rigo, P. Viglino and G. Rotilio, Biochem. Biophys. Res. Commun., 63 (1975) 1013.
50 S. Ozaki, J.Hirose and Y. Kidani, Inorg. Chem., 27 (1988) 3746.
51 K.G. Strothkamp and S.J. Lippard, Biochemistry, 20 (1981) 7488.
52 A.E.G. Cass, H.A.O. Hill, V. Hasemann and J.T. Johansen, Carlsberg Res. Commun., 43 (1978) 439.
53 J.A. Fee and R.L. Ward, Biochem. Biophys. Res. Commun., 71 (1976) 427.

54 G.D. Lawrence and D.T. Sawyer, Biochemistry, 18 (1979) 3045.
55 R.A. Hallewell, R. Mills, P. Tekamp-Olson, R. Blacher, S. Rosenberg, F. Otting, F.R. Masiarz and C.J. Scandella, Biotechnology, 5 (1987) 363.
56 R.A. Hallewell, F.R. Masiarz, R.C. Najarian, J.P. Puma, M.R. Quiroga, A. Randolph, R. Sanchez-Pescador, C.J. Scandella, B. Smith, K.S. Steimer and G.T. Mullenbach, Nucl. Acids Res., 13 (1985) 2017.
57 R.A. Hallewell, K. Imlay, I. Laria, C. Gallegos, N.M. Fong, B. Irvine, E.D. Getzoff, J.A. Tainer, D. Cabelli, B.H.J. Bielski, P. Olson, G.T. Mullenbach and L.S. Cousens, 1989, submitted for publication.
58 L. Banci, I. Bertini, C. Luchinat and R.A. Hallewell, Ann. N.Y. Acad. Sci., 542 (1988) 37.
59 I. Bertini, L. Banci, C. Luchinat, B.H.J. Bielski, D.E. Cabelli, G.T. Mullenbach and R.A. Hallewell, J. Am. Chem. Soc., 111 (1989) 714.
60 W.F. Beyer, I. Fridovich, G.T. Mullenbach and R.A. Hallewell, J. Biol. Chem., 262 (1987) 11182.
61 L. Banci, I. Bertini, C. Luchinat and R.A. Hallewell, J. Am. Chem. Soc., 110 (1988) 3629.
62 (a) Chiron Corporation, Emeryville, CA, unpublished results, 1989.
(b) I. Bertini, unpublished results, 1989.
63 I. Bertini and A. Scozzafava, in H. Sigel (Ed.), Metal Ions in Biological Systems, Vol. 12, Marcel Dekker, New York, 1981, p. 31.
64 B.J. Hathaway and A.A.G. Tomlinson, Coord. Chem. Rev., 5 (1970) 1.
65 K. Karlin and J. Zubjeta (Eds.), Copper Coordination Chemistry, Biochemical and Inorganic Perspectives, Adenine Press, New York, 1983; Biological and Inorganic Copper Chemistry, Vols. I and II, Adenine Press, New York, 1986.
66 A.B.P. Lever, Inorganic Electronic Spectroscopy, 2nd edn., Elsevier, Amsterdam, 1984.
67 B.L. Vallee, B. Holmquist, in D.W. Darnall and M.G. Wilkins (Eds.), Advances in Inorganic Biochemistry, Elsevier North-Holland, New York, Vol. 2, 1980, p. 27.
68 C.J. Hawkins, Absolute Configuration of Metal Complexes, Wiley, New York, 1971.
69 A. Abragam and B. Bleaney, Electron Paramagnetic Resonance of Transition Ions, Clarendon Press, Oxford, 1970.
70 A. Bencini and D. Gatteschi, Transition Met. Chem., 8 (1982) 1.
71 L. Kevan and L.D. Kispert, Electron Spin Double Resonance Spectroscopy, Wiley, New York, 1976.
72 J. Huttermann and R. Kappl, in H. Sigel (Ed.), Metal Ions in Biological Systems, Vol. 22, Marcel Dekker, New York, 1987, p. 1.
73 Y.D. Tsvetkov and S.A. Dikanov, in H. Sigel (Ed.), Metal Ions in Biological Systems, Vol. 22, Marcel Dekker, New York, 1987, p. 207.
74 I. Bertini and C. Luchinat, NMR of Paramagnetic Molecules in Biological Systems, Benjamin/Cummings, Menlo Park, CA, 1986.
75 I. Bertini, C. Luchinat and L. Messori, in H. Sigel (Ed.), Metal Ions in Biological Systems, Vol. 21, Marcel Dekker, New York, 1987, p. 47.
76 I. Bertini, F. Briganti and C. Luchinat, in N. Niccolai and G. Valensin (Eds.), Advanced Magnetic Resonance Techniques in Systems of High Molecular Complexity, Birkhauser, Basle, 1986, p. 165.
77 L. Banci, I. Bertini and C. Luchinat, Magn. Reson. Rev., 11 (1986) 1.
78 M.W. Pantoliano, J.S. Valentine and L.A. Nafie, J. Am. Chem. Soc., 104 (1982) 6310, and references cited therein.
79 K. Krogh-Jespersen and H.J. Schugar, Inorg. Chem., 23 (1984) 4390.
80 (a) R. Bauer, I. Demeter, V. Hasemann and J.T. Johansen, Biochem. Biophys. Res. Commun., 94 (1980) 1296.

(b) M.J. Bjerrum, P. Kofod, R. Bauer and E. Danielsen, in G. Czapski (Ed.) Proc. 5th Conf. Superoxide and Superoxide Dismutase, Jerusalem, 1989.
81 (a) T.G. Fawcett, E.E. Bernarducci, K. Krogh-Jespersen and H.J. Schugar, J. Am. Chem. Soc., 102 (1980) 2598.
(b) E. Bernarducci, W.F. Schwindinger, J.L. Hughey, K. Krogh-Jespersen and H.J. Schugar, J. Am. Chem. Soc., 103 (1981) 1686.
(c) H.J. Schugar, in K. Karlin and J. Zubjeta (Eds.), Copper Coordination Chemistry, Biochemical and Inorganic Perspectives, Adenine Press, New York, 1983, p. 43.
(d) E. Bernarducci, P.K. Bharadwaj, K. Krogh-Jespersen and H.J. Schugar, J. Am. Chem. Soc., 105 (1983) 3860.
82 J.A. Fee and W.D. Philips, Biochim. Biophys. Acta, 412 (1975) 26.
83 I. Bertini, G. Lanini, C. Luchinat, L. Messori, R. Monnanni and A. Scozzafava, J. Am. Chem. Soc., 107 (1985) 4391.
84 I. Bertini, C. Luchinat and A. Scozzafava, J. Am. Chem. Soc., 102 (1980) 7349.
85 I. Bertini, E. Borghi, C. Luchinat and A. Scozzafava, J. Am. Chem. Soc., 103 (1981) 7779.
86 G. Rotilio, A. Finazzi-Agro, L. Calabrese, F. Bossa, P. Guerrieri and B. Mondovi, Biochemistry, 10 (1971) 616.
87 M. Pantoliano, P.J. McDonnell and J.S. Valentine, J. Am. Chem. Soc., 101 (1979) 6454.
88 R.G. Brigg and J.A. Fee, Biochim. Biophys. Acta, 537 (1978) 86.
89 R.A. Liebermann, R.H. Sands and J.A. Fee, J. Biol. Chem., 257 (1982) 336.
90 L. Banci, I. Bertini, C. Luchinat, R.A. Hallewell and M.S. Viezzoli, Eur. J. Biochem., 184 (1989) 125.
91 H.L. Van Camp, R.H. Sands and J.A. Fee, Biochim. Biophys. Acta, 704 (1982) 75.
92 J. Huttermann, R. Kappl, L. Banci and I. Bertini, Biochim. Biophys. Acta, 956 (1988) 173.
93 H.L. Van Camp, R.H. Sands and J.A. Fee, J. Chem. Phys., 75 (1981) 2098.
94 J.A. Fee, J. Peisach and W.B. Mims, J. Biol. Chem., 256 (1981) 1910.
95 S.H. Koenig and R.D. Brown III, in H. Sigel (Ed.), Metal Ions in Biological Systems, Vol. 21, Marcel Dekker, New York, 1987, p. 229.
96 I. Solomon, Phys. Rev., 99 (1955) 559.
97 I. Bertini, F. Briganti, C. Luchinat, M. Mancini and G. Spina, J. Magn. Reson., 63 (1985) 41.
98 P. Gaber, R. Brown III, S.H. Koenig and J.A. Fee, Biochim. Biophys. Acta, 271 (1972) 1.
99 N.J. Blackburn, S.S. Hasnais, G.P. Diakun, P.F. Knowles, N. Binsted and C.D. Garner, Biochem. J., 213 (1983) 765.
100 L. Banci, I. Bertini, C. Luchinat, R. Monnanni and A. Scozzafava, Inorg. Chem., 27 (1988) 107.
101 L. Banci, I. Bertini, C. Luchinat, A. Scozzafava and P. Turano, Inorg. Chem., 28 (1989) 2377.
102 G. Rotilio, L. Morpurgo, C. Giovagnoli, L. Calabrese and B. Mondovì, Biochemistry, 11 (1972) 2187.
103 L. Banci, I. Bertini, C. Luchinat and A. Scozzafava, J. Am. Chem. Soc., 109 (1987) 2328.
104 I. Bertini, C. Luchinat, C. Owens and R.S. Drago, J. Am. Chem. Soc., 109 (1987) 5208.
105 I. Bertini, L. Banci and C. Luchinat, Am. Chem. Soc., Symp. Ser., 372 (1988) 70.
106 I. Morgenstern-Badarau, D. Cocco, A. Desideri, G. Rotillo, J. Jordanov and N. Dupré, J. Am. Chem. Soc., 108 (1986) 300.
107 L. Banci, I. Bertini and C. Luchinat, Struct. Bonding, 72 (1990) 113.
108 L.-J. Ming, L. Banci, C. Luchinat, I. Bertini and J.S. Valentine, Inorg. Chem., 27 (1988) 4458.

109 L.-J. Ming, L. Banci, C. Luchinat, I. Bertini and J.S. Valentine, Inorg. Chem., 27 (1988) 728.
110 H.P.W. Gottlieb, M. Barfield and D.M. Doddrell, J. Chem. Phys., 67 (1977) 3785.
111 L. Banci, I. Bertini, C. Luchinat, M. Piccioli, A. Scozzafava and P. Turano, Inorg. Chem., in press.
112 M. Gueron, J. Magn. Reson., 19 (1975) 58.
113 A.J. Vega and D. Fiat, Mol. Phys., 31 (1976) 347.
114 L. Banci, I. Bertini, C. Luchinat and M.S. Viezzoli, Inorg. Chem., in press.
115 (a) J.H. Noggle and R.E. Shirmer, The Nuclear Overhauser Effect, Academic Press, New York, 1971.
(b) D. Neuhaus and M. Williamson, The Nuclear Overhauser Effect in Structural and Conformational Analysis, VCH, New York, 1989.
116 S. Ramaprasad, R.D. Johnson and G.N. La Mar, J. Am. Chem. Soc., 105 (1983) 7205.
117 S. Ramaprasad, R.D. Johnson and G.N. La Mar, J. Am. Chem. Soc., 106 (1984) 5330.
118 W.O. Parker, Jr., M.J. Chatfield and G.N. La Mar, Biochemistry, 28 (1989) 1517.
119 L. Banci, I. Bertini, C. Luchinat and A. Scozzafava, J. Biol. Chem., 264 (1989) 9742.
120 D.P. Malinowski and I. Fridovich, Biochemistry, 18 (1979) 5909.
121 O. Bermingham-McDonough, D. Mota de Freitas, A. Kunamoto, J.E. Saunders, D.M. Blech, C.L. Borders, Jr., and J.S. Valentine, Biochem. Biophys. Res. Commun., 108 (1982) 1376.
122 D. Mota de Freitas, C. Luchinat, L. Banci, I. Bertini and J.S. Valentine, Inorg. Chem., 26 (1987) 2788.
123 W.F. Beyer, Jr., Y. Wang and I. Fridovich, Biochemistry, 25 (1986) 6084.
124 D. Mota de Freitas and J.S. Valentine, Biochemistry, 23 (1984) 2079.
125 J.A. Cowan, R.K. Upmacis, D.N. Beratan, J.N. Onuchic and H.B. Gray, Ann. N.Y. Acad. Sci., 550 (1988) 68.
126 I. Bertini, C. Luchinat and R. Monnanni, J. Am. Chem. Soc., 107 (1985) 2178.
127 T.H. Moss and J.A. Fee, Biochem. Biophys. Res. Commun., 66 (1975) 799.
128 N.J. Blackburn, S.S. Hasnain, N. Binsted, G.P. Diakun, C.D. Garner and P.F. Knowles, Biochem. J., 219 (1984) 985.
129 I. Bertini, L. Banci, C. Luchinat and M. Piccioli, unpublished results, 1989.
130 R. Osman and H. Basch, J. Am. Chem. Soc., 106 (1984) 5710.
131 R. Osman, Enzyme, 36 (1986) 32.
132 M. Rosi, A. Sgamellotti, F. Tarantelli, I. Bertini and C. Luchinat, Inorg. Chim. Acta, 107 (1985) L21.
133 M. Rosi, A. Sgamellotti, F. Tarantelli, I. Bertini and C. Luchinat, Inorg. Chem., 25 (1986) 1005.
134 G. Rotilio, L. Morpurgo, C. Giovagnoli, L. Calabrese and B. Mondovì, Biochemistry, 11 (1972) 2187.
135 M.A. Symonyan and R.M. Nalbandyan, FEBS Lett., 28 (1972) 22.
136 R.C. Bray, H.S. Cockle, E.M. Fielden, P.B. Roberts, G. Rotilio and L. Calabrese, Biochem. J., 139 (1974) 43.
137 D. Klug, J. Rabani and I. Fridovich, J. Biol. Chem., 95 (1972) 2786.
138 E.M. Fielden, P.B. Roberts, R.C. Bray and G. Rotilio, Biochem. Soc. Trans., 1 (1973) 53.

139 G. Rotilio, L. Morpurgo, L. Calabrese and B. Mondovì, Biochim. Biophys. Acta, 302 (1973) 229.
140 E.K. Hodgson and I. Fridovich, Biochemistry, 14 (1975) 5294.
141 I. Bertini, C. Luchinat, M.S. Viezzoli and Y. Wang, Arch. Biochem. Biophys., 269 (1989) 586.
142 H.J.R. Fuchs and C.L. Borders, Jr., Biochem. Biophys. Res. Commun., 116 (1983) 1107.
143 P.J. Horton, C.L. Borders, Jr., and W.F. Beyer, Jr., Arch. Biochem. Biophys., 269 (1989) 114.